Available online at www.sciencedirect.com
ScienceDirect
Tetrahedron
Tetrahedron 63 (2007) 11724–11732

# A $Cu^{2+}$ protein cavity mimicking fluorescent chemosensor for selective $Cu^{2+}$ recognition: tuning of fluorescence quenching to enhancement through spatial placement of anthracene unit

Subodh Kumar,* Prabhpreet Singh and Sukhdeep Kaur

*Department of Chemistry, Guru Nanak Dev University, Amritsar 143005, Punjab, India*

Received 12 March 2007; revised 15 August 2007; accepted 30 August 2007
Available online 6 September 2007

**Abstract**—Four new fluoroionophores possessing four ligating sites (2S+2N) and an essential hydrophobic environment, as prevailing in the plastocyanin and rusticyanin proteins, have been synthesized. In these PET fluoroionophores, the position of fluorophore anthracene moiety effectively modulates the $Cu^{2+}$ induced emission properties (quenching vs enhancement) of the fluorophore. The addition of $Cu^{2+}$ to solution of receptor with anthracene moiety in its center caused quenching in emission intensity through photoinduced fluorophore-to-metal *electron transfer* mechanism and in cases where anthracene is present at terminus nitrogen, the emission intensities increased by nearly 1000% due to inhibition of the photoinduced electron transfer from receptor-to-fluorophore in the presence of $Cu^{2+}$ ions. The hydrophobic environment created by various aromatic rings clearly manifested the stability of fluorescence of these molecules above pH 2.0 and their $Cu^{2+}$ complexes above pH 4. The application of such fluoroionophores has been elaborated for building OR and AND logic gates.


## 1. Introduction

Fluorescent chemosensors for the detection and measurement of metal ions, especially for cations of biological interest such as $Na^+$, $Ca^{2+}$, $Cu^{2+}$, and $Zn^{2+}$ are actively investigated.[1] Amongst the soft transition metal ions, $Cu^{2+}$ is third in abundance (after $Fe^{2+}$ and $Zn^{2+}$) in the human body and plays an important role in various biological systems. The design and synthesis of chemosensors for $Cu^{2+}$ constitute a very active area of research as a result of the demand for more sensitive and selective chemosensors for in vitro and in vivo purposes.[2,3]

Although $Cu^{2+}$ is a significant metal pollutant due to its widespread use,[2,3] it is also an essential element for life because alterations in its cellular homeostasis are connected to serious neurodegenerative diseases like Alzheimer's, Menke's, and Wilson's diseases.[4]

The synthetic $Cu^{2+}$ selective fluoroionophores so far reported[5–17] have amide units as an integral part of the ionophore and $Cu^{2+}$ is known to trigger the hydrolysis of the amide linkages affecting the stability of these amide based sensors. In nature, blue copper proteins play a key role in long range inter- and intraprotein electron transfer[18,19] and are characterized by high reduction potentials, rapid transfer rates, and unique spectral features compared to normal tetragonal copper complexes. In rusticyanin ($2\times N+2\times S$), the four ligating atoms are arranged around copper in a distorted tetrahedral arrangement but have high acid stability as the copper binding site is located within a hydrophobic region at one end of the molecule, surrounded by a number of aromatic rings and hydrophobic residues. This conformation probably contributes to the acid stability of the copper site, since the close association of aromatic rings with the histidine ligand would sterically hinder their dissociation from copper.[19b]

For most of the reported $Cu^{2+}$ fluorescent sensors, the binding of the metal ion causes a quenching of the fluorescence emission.[15] Due to sensitivity reasons, fluoroionophores showing fluorescence enhancement as a result of metal ion binding are to be favored over those exhibiting fluorescence quenching. A number of fluoroionophores, in which the binding of a $Cu^{2+}$ ion causes an increase in the fluorescence[16], have been reported. Among those reported, $Cu^{2+}$ binding resulting in the inhibition of photoinduced electron transfer (PET) in the fluoroionophores has been an important mechanism, with the metal ionophore located in the electron donor.

In the present investigations, bearing in mind the structural features of the active cavity in $Cu^{2+}$ proteins in the cases of plastocyanin and rusticyanin having two N and two S binding sites and the additional stability provided by aromatic rings in the case of rusticyanin, the acyclic

* Corresponding author. Fax: +91 183 2258820; e-mail: subodh_gndu@yahoo.co.in

0040–4020/$ - see front matter © 2007 Elsevier Ltd. All rights reserved.
doi:10.1016/j.tet.2007.08.101

fluoroionophores **3**,[17a] **8**, **9**, and **12**, possessing 2-aminothiophenol units as ligating sites placed at the 9,10-position of anthracene or at the 1,4 position of the substituted phenylene rings, have been designed. In the case of **3**, the anthracene moiety is part of the main skeleton of the fluoroionophore and is positioned perpendicular to the ligating sites. As a result, the anthracene unit faces the cavity of the ionophore and thus increases the sensitivity and selectivity toward $Cu^{2+}$ through coordination but causes >40% fluorescence quenching on addition of ≥9 μM $Cu^{2+}$. However, the presence of anthracene ring as an appendage at the terminus in the case of **8**, **9**, and **12** results in a decrease in coordination of anthracene moiety with $Cu^{2+}$ and causes an increase in emission, though it adversely affects the stability of the fluorophore–$Cu^{2+}$ complex and its selectivity.

## 2. Results and discussion

### 2.1. Synthesis of fluoroionophores 3, 8, 9, and 12

The phase transfer catalyzed (NaH–DMF–TBA $HSO_4$) nucleophilic substitution of **1**[20] with 2-aminothiophenol **2** provided **3** as a fluorescent yellow solid (85%), mp 186 °C, FAB mass *m/z* 452 ($M^+$+H) (Scheme 1).

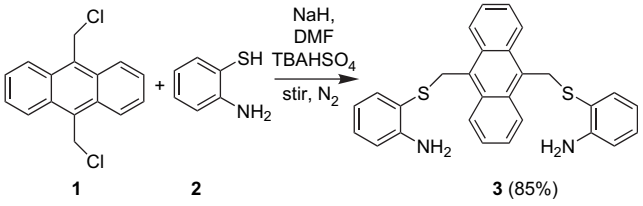


**Scheme 1**.

The phase transfer catalyzed (NaH–DMF–TBA $HSO_4$) nucleophilic substitutions of dibromides **4** and **5** with 2-aminothiophenol provided **6**, white solid (60%), mp 101–103 °C, (lit. mp 104–106 °C),[21] FAB mass *m/z* 353 ($M^+$+H) and **7**, white solid (70%), mp 148–149 °C, FAB mass *m/z* 412 ($M^+$) (Scheme 2), respectively. The solution of **6** and anthracene-9-aldehyde in dry THF was stirred for 2 days and was then reduced with $NaBH_4$–$I_2$ mixture. The reaction mixture on work-up and column chromatography gave yellow solid **8** (20%), mp 122–123 °C, FAB mass *m/z* 542 ($M^+$) (Scheme 2).

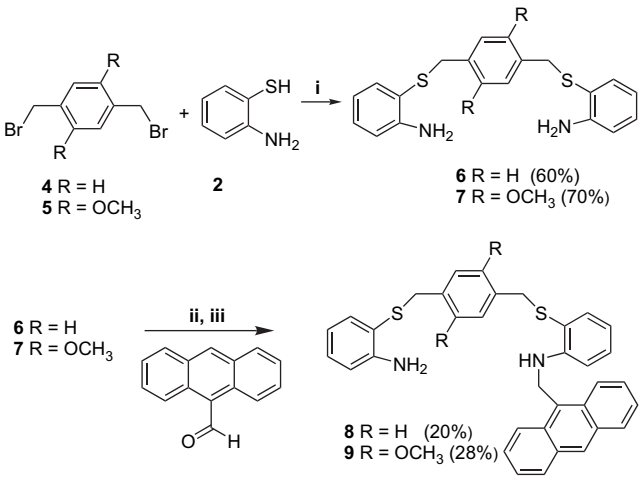


(i) NaH-DMF, TBA $HSO_4$, $N_2$, stir (ii) THF, $MgSO_4$, stir (iii) $NaBH_4$, $I_2$, THF,reflux

**Scheme 2**.

The appearance of two 2H singlets at δ 3.58 and 3.75 due to $SCH_2$ protons and two 2H doublets at 6.69 and 6.80 due to benzene ArH; 2H and 1H exchangeable signals at δ 4.13 and 5.21 in its $^1$H NMR spectrum along with other signals and 26 signals in $^{13}$C NMR spectrum show that **8** is unsymmetrical and only one $NH_2$ of **6** is anthracenylmethylated and confirm the structure **8** for this compound. Similarly, diamine **7** on reaction with anthracene-9-aldehyde and subsequent reduction gave **9** (28%), mp 124–125 °C, FAB mass 602 ($M^+$).

In order to rationalize the difference in contribution of the π-cloud of naphthalene and anthracene units in coordination with $Cu^{2+}$, when placed as part of the main skeleton of the receptor, the naphthalene-based fluoroionophore **12** was also synthesized. The nucleophilic substitution of 1,4-bis-(chloromethyl)-naphthalene (**10**) with 2-aminothiophenol (**2**) gave **11**, white solid (55%), mp 76–78 °C, FAB mass *m/z* 402 ($M^+$), which on reductive anthracenylmethylation gave **12** (27%), mp 135–137 °C, FAB mass *m/z* 592 ($M^+$) (Scheme 3).

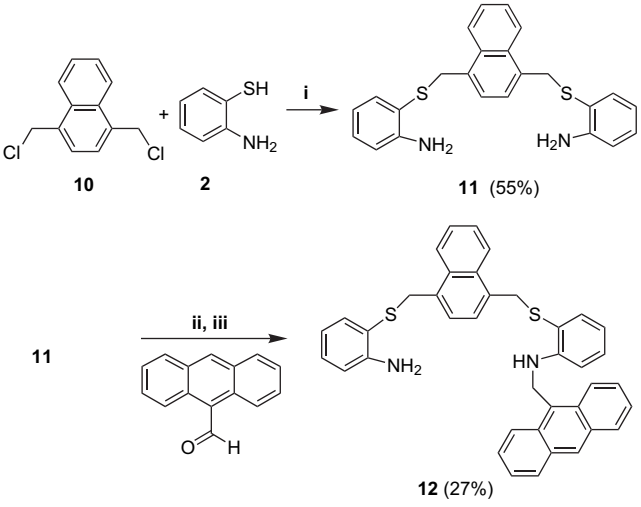


**Scheme 3**.

### 2.2. Photophysical behavior of fluoroionophores 3, 8, 9, and 12

The fluoroionophore **3** in its UV–vis spectrum shows $\lambda_{max}$ at 411, 390, 371, and 303 nm, whereas **8**, **9**, and **12** (50 μM) in $CH_3CN$–$H_2O$ (4:1 v/v), in their UV–vis spectra displayed $\lambda_{max}$ at 387, 365, and 348 nm typical for anthracene unit. The UV–vis spectra of fluoroionophores **8**, **9**, and **12** thus show a blue shift of 23–25 nm for all three absorption bands in comparison with fluoroionophore **3**. The solutions of these fluoroionophores (5 μM) [$CH_3CN$–$H_2O$, 4:1] on excitation at $\lambda_{ex}$ 365 nm[22] exhibited fluorescence maxima at $\lambda_{max}$ 412 nm, with two shoulders at 393 and 439 nm, typical of anthracene unit. In the concentration range 1–500 μM, the fluorescence of **3**, **8**, **9**, and **12** remained directly proportional

to their concentrations. This linear increase in fluorescence with concentration of **3**, **8**, **9**, and **12** indicates that these fluoroionophores are not susceptible to self-quenching or to aggregation processes in this concentration range.

**2.2.1. Photophysical behavior of fluoroionophore 3.** Fluoroionophore **3** possesses two Ar-$NH_2$ units and would undergo protonation in the presence of acid to inhibit photoinduced electron transfer (PET) from amine nitrogen to excited anthracene unit. So, first, a solution of **3** (5 μM) ($CH_3CN$–$H_2O$, 4:1) was titrated with a standard acid and base. No change of the intense characteristic emission of anthracene was observed over the pH range (14–3.8). However, on further lowering the pH, the intensity of emission band began to increase at pH=3.8 and fluorescence was completely increased (nearly three times) at pH=2. The plot of FI against pH displays a sigmoid profile (Fig. 1).

Thus, fluoroionophore **3** shows 'OFF–ON' phenomena under acidic conditions. The spectral fitting of the pH titration data shows p$K_a$=2.6±0.1 for **3**. In preliminary fluorescence studies, fluoroionophore **3** (5 μM) at pH 7.0 (HEPES 10 mM) in $CH_3CN$–$H_2O$ (4:1 v/v) in the presence of 500 μM metal ions shows fluorescence quenching with $Cu^{2+}$ while other metal ions viz. $Ni^{2+}$, $Cd^{2+}$, $Zn^{2+}$, $Hg^{2+}$, and $Pb^{2+}$ do not affect the fluorescence.

The plot of fluorescence intensity of **3** (5 μM) [$CH_3CN$–$H_2O$ (4:1), HEPES 10 mM] at 415 nm versus concentration of $Cu^{2+}$ exhibits a gradual decrease in fluorescence intensity with the increase in concentration of $Cu^{2+}$ between 1 and 8 μM, after which the fluorescence levels off and a plateau is achieved (Fig. 2b). Therefore, **3** can estimate 1–8 μM of $Cu^{2+}$ through fluorescence spectroscopy and undergoes ~40% fluorescence quenching (Fig. 2a). The spectral fitting of the data for **3**·$Cu(NO_3)_2$ titration shows the formation of $M_2L$ complex with log $\beta_{M_2L} = 15.20 \pm 1.46$.

A similar titration experiment was carried out on UV–vis spectrophotometer at a higher concentration of **3** (20 μM) to further explore the possibility of these fluoroionophores to act as chromogenic sensors for $Cu^{2+}$. The solutions containing fluoroionophore **3** (20 μM) and varied concentrations of $Cu^{2+}$ (1–200 μM) were prepared in $CH_3CN$–$H_2O$ (4:1) at pH ~7 (HEPES 10 mM) and their UV–vis spectra recorded (Fig. 3a). The plot of absorbance at 415 nm versus the concentration of $Cu^{2+}$ displays a linear decrease in the absorbance from 1 to 40 μM (0.1–2.0 equiv) and then a plateau is achieved (Fig. 3b). It was observed that the light yellow color of the fluoroionophore disappears on addition of $Cu^{2+}$. The fluoroionophore **3** can therefore be used for the selective estimation of 1–40 μM $Cu^{2+}$ by UV–vis spectroscopy.

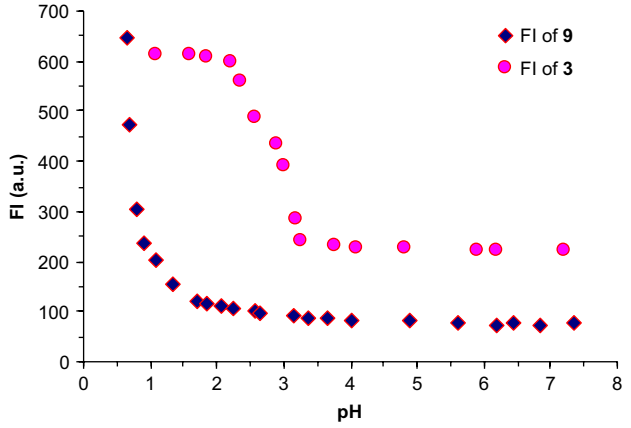


**Figure 1**. The plot of change in FI of **3** (5 μM, $CH_3CN$–$H_2O$, 4:1) versus pH at 412 nm. The change in FI of **9** (1 μM, $CH_3CN$–$H_2O$, 4:1) versus pH at 412 nm is also given for comparison.

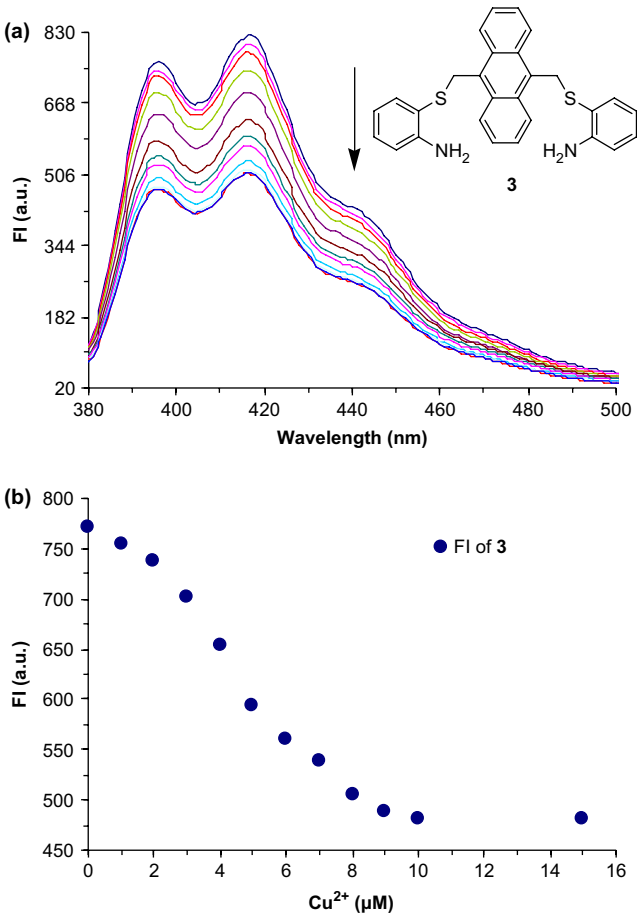


**Figure 2**. (a) The effect of $Cu^{2+}$ on the fluorescence spectrum of **3** showing fluorescence quenching and (b) the plot of fluorescence intensities of **3** (●) (5 μM) at 25±1 °C, pH 6.90 (HEPES 10 mM) versus $Cu^{2+}$ concentration in $CH_3CN$–$H_2O$.

**2.2.2. Photophysical behavior of fluoroionophores 8, 9, and 12.** Like other amine-based fluorescent sensors, **8**, **9**, and **12** are also pH sensitive. The pH titration of **9** (5 μM) ($CH_3CN$–$H_2O$, 4:1) showed that the fluorescence intensity of **9** remained unaffected between pH 14 and 2. On lowering the pH below 2.0, the fluorescence intensity increased sharply and below pH 1.0, it went off scale (Fig. 1). Similarly, fluorescence of **8** and **12** remained stable up to pH 2.0 and on further lowering the pH resulted in sharp fluorescence enhancement. Thus, fluoroionophores **8**, **9**, and **12** also show 'OFF–ON' phenomena under acidic conditions. The effect of hydrophobic environment in **8**, **9**, and **12** (where the anthracene ring is placed at the termini) is clearly manifested into the stability of fluorescence of these molecules above pH 2.0 and at pH<2 the protonation of amine NH inhibits PET phenomenon and a sharp increase in emission is

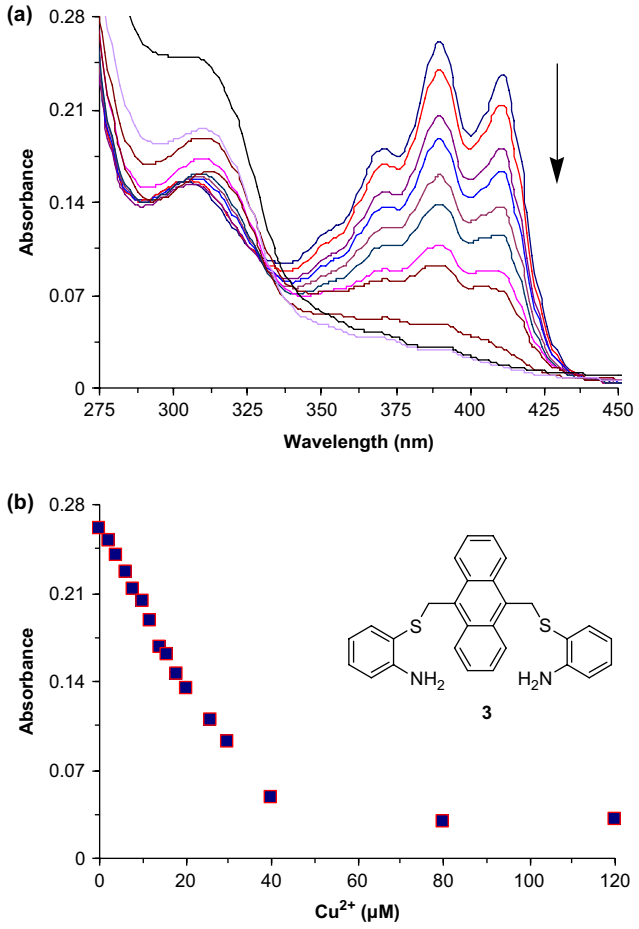


**Figure 3**. (a) The effect of addition of $Cu^{2+}$ on the absorption spectrum of **3** (20 μM) at 25±1 °C, pH 6.90 (HEPES 10 mM) in $CH_3CN$–$H_2O$ (4:1). (b) The plot of absorbance of **3** (■) versus $Cu^{2+}$ concentration in $CH_3CN$–$H_2O$.

observed. The spectral fitting of the pH titration data shows $pK_a$=0.91±0.11 for **8**, 0.8±0.07 for **9**, and 1.5±0.05 for **12**. In these fluoroionophores, aromatic amine NH units give $pK_a \leq 1.5$, which is significantly lower than the $pK_a$ of aniline[23] ($pK_a$=4.63 in water). Possibly, in **8**, **9**, and **12** the hydrophobic environment created by the aromatic rings makes the protonation more difficult.

In preliminary fluorescence studies the addition of $Cu^{2+}$ (500 μM) to solution of **8**, **9**, and **12** (5 μM) [$CH_3CN$–$H_2O$ (4:1), HEPES buffer (10 mM)] caused immediate increase in fluorescence intensity by nearly 10 times and remained stable (±5%) for even 6 h. On addition of EDTA (500 μM), FI of this solution reversed back to original FI of the fluorophore. Other heavy metal ions (500 μM) affected fluorescence intensity only marginally (Fig. 4). Also, the presence of alkali and alkaline earth metal ions does not affect the fluorescence of these fluoroionophores. These preliminary results clearly show that **8**, **9**, and **10** have selectively $Cu^{2+}$ induced fluorescence enhancement.

Fluoroionophores **8** and **12** [5 μM, $CH_3CN$–$H_2O$ (4:1), HEPES buffer (10 mM), pH 6.9] on gradual increase in $Cu(NO_3)_2$ concentration showed a gradual increase in fluorescence (Fig. 5a). The plot of fluorescence intensity of **8** versus concentration of $Cu(NO_3)_2$ exhibited a sharp increase in fluorescence up to 10 equiv of $Cu^{2+}$ and then a slow change

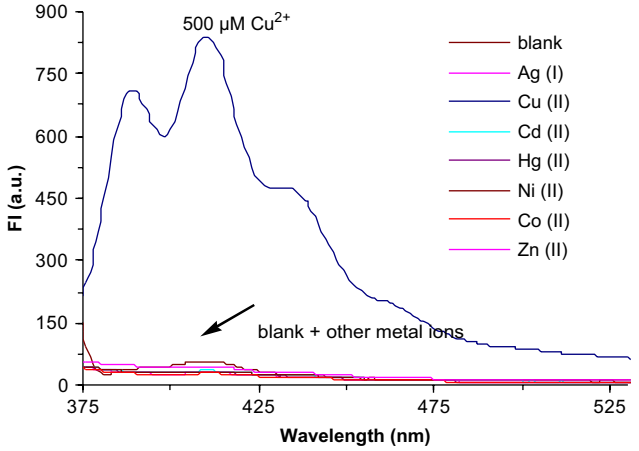


**Figure 4**. The effect of various metal ions (500 μM) on the fluorescence of **8** (5 μM).

in fluorescence up to 80 equiv (400 μM) of $Cu^{2+}$ took place, and a plateau was achieved. The spectral fitting of the data shows the formation of $ML_2$ and $M_2L$ complexes with $\log \beta_{ML_2} = 10.4 \pm 0.3$ and $\log \beta_{M_2L} = 7.6 \pm 0.2$. On initial addition of $Cu(NO_3)_2$, $ML_2$ complex is formed, which achieves a maximum concentration (40%) at 20 equiv of $Cu(NO_3)_2$. At this concentration, a small amount of $M_2L$ (5%) is also observed. Furthermore, even on the addition of 100 equiv of $Cu(NO_3)_2$, only 50% of $M_2L$ along with 20%

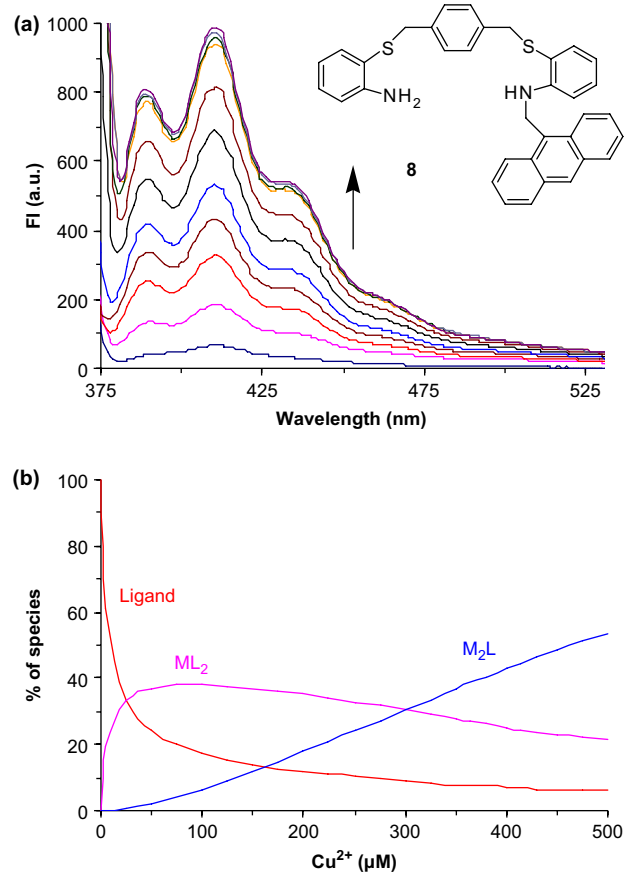


**Figure 5**. The effect of $Cu^{2+}$ on the fluorescence spectrum of **8** showing fluorescence enhancement. (b) The speciation diagram showing % distribution of $ML_2$ and $M_2L$ species with fluoroionophores **8** (5 μM, $CH_3CN$) on addition of $Cu(NO_3)_2$ determined fluorometrically.

$ML_2$ is observed (Fig. 5b).[24] Similarly, **12** with $Cu^{2+}$ forms $ML_2$ and $M_2L$ complexes with $\log \beta_{ML_2} = 9.1 \pm 0.1$ and $\log \beta_{M_2L} = 7.2 \pm 0.3$ and points to an insignificant contribution of the central naphthalene ring in cation–π interaction.

A solution of **9** (5 μM) [pH 6.9, HEPES (10 mM), $CH_3CN$–$H_2O$ (4:1)] on addition of $Cu(NO_3)_2$ showed FE at both $\lambda_{max}$ 415 nm and 480 nm, which gradually increased with increasing $Cu(NO_3)_2$ concentration. In the case of anthracene derivatives, such longer wavelength emission bands usually arise due to excimer formation, but here the reason for appearance of this emission could not be ascertained (Fig. 6a). The intensity of emission band at 480 nm along with the monomer emission band increased with the increase in the concentration of $Cu(NO_3)_2$ and reached almost maxima at 500 μM $Cu(NO_3)_2$. The spectral fitting of the data shows the formation of $ML_2$ and $M_2L$ complexes with $\log \beta_{ML_2} = 9.8 \pm 0.3$ and $\log \beta_{M_2L} = 7.5 \pm 0.2$ (Fig. 6b).

To further explore the possibility of these fluoroionophores to act as chromogenic sensor for $Cu^{2+}$, the effect of $Cu^{2+}$ on the UV–vis behavior of **8**, **9**, and **12** has been studied. Fluoroionophores **8**, **9**, and **12** (50 μM) showed significant lowering in absorbance on the addition of $Cu(NO_3)_2$.

The plot of absorbance at 367 nm versus $Cu^{2+}$ concentration displays a linear decrease in the absorbance up to 10 equiv of $Cu(NO_3)_2$ and then a plateau is achieved (Fig. 7b). On addition of $Cu(NO_3)_2$ the solution became bright yellow in color and a new broad band emerged at around 410 nm (Fig. 7a). The absorbance of this band gradually increased with increase in the concn of $Cu(NO_3)_2$ between 50 and 1000 μM (1–20 equiv). Similarly, **9** and **12**, on addition of $Cu(NO_3)_2$, showed a decrease in absorbance at 348, 365, and 387 nm due to the anthracene unit and increase in absorbance between 410 and 480 nm. This decrease in absorbance due to the anthracene unit and the simultaneous increase in absorbance between 400 and 480 nm regions could be attributed to metal–ligand complex formation. However, the lowering in absorbance (~30–40%) is significantly less than that in the case of fluoroionophore **3** (~80%). The spectral fitting of the UV–vis data also shows the formation of $ML_2$ and $M_2L$ complexes with $\log \beta_{ML_2} = 10.1 \pm 0.1$, $\log \beta_{M_2L} = 7.1 \pm 0.3$ for **8**, $\log \beta_{ML_2} = 9.2 \pm 0.1$, $\log \beta_{M_2L} = 7.2 \pm 0.3$ for **9**, and $\log \beta_{ML_2} = 9.2 \pm 0.1$, $\log \beta_{M_2L} = 7.1 \pm 0.3$ for **12**.

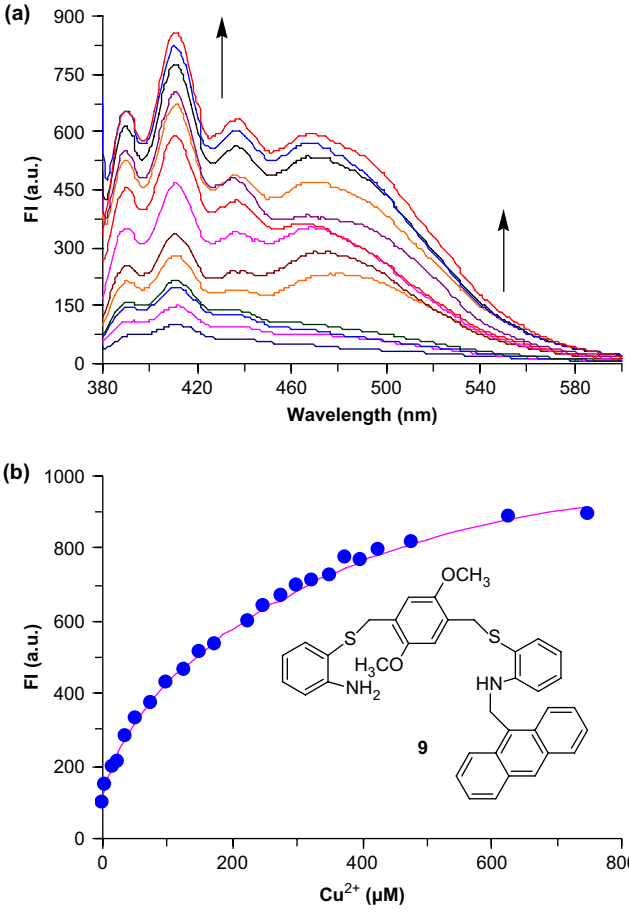


**Figure 6**. (a) The effect of $Cu^{2+}$ on the fluorescence of **9** and (b) curve fitting of change in FI of **9** (5 μM) at 412 nm on addition of $Cu(NO_3)_2$ (●) experimental points, (—) fitted line.

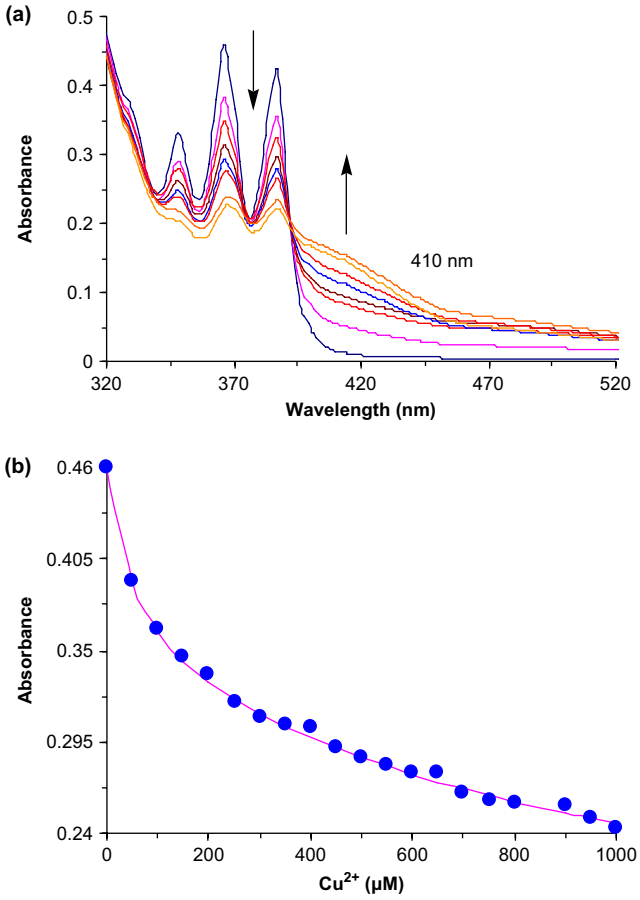


**Figure 7**. (a) The effect of addition of $Cu^{2+}$ on the absorption spectrum of **8** (50 μM) at 25±1 °C, pH 6.90 (HEPES 10 mM) in $CH_3CN$–$H_2O$ (4:1). (b) Curve fitting of change in FI of **8** (50 μM) at 412 nm on addition of $Cu(NO_3)_2$ (●) experimental points, (—) fitted line.

## 2.3. The nature of metal induced fluorescence quenching and/or enhancement in fluoroionophores 3, 8, 9, and 12

The fluorescence quenching in **3** on addition of $Cu^{2+}$ could be attributed to the strong interaction of anthracene with $Cu^{2+}$, which leads to easy electron transfer. The uncomplexed sensors **8**, **9**, and **12** are not fluorescent, as the

photoexcited fluorophore is deactivated by a nonradiative mode through the transfer of an electron from the highly reducing proximate secondary amine group. Following metal incorporation (in this case $Cu^{2+}$), the metal–ligand interaction decreases the amine oxidation potential drastically and prevents the electron transfer. As a consequence, the intense and characteristic anthracene emission is largely restored. Therefore, on shifting the anthracene ring from center of the molecule in fluoroionophore **3** to the terminal in **8**, **9**, and **12**, the $Cu^{2+}$ induced fluorescence quenching is reversed to fluorescence enhancement.

The pH titrations of 1:1 solutions of **8**-$Cu^{2+}$, **9**-$Cu^{2+}$, and **12**-$Cu^{2+}$ complexes showed that the change in fluorescence achieved by the addition of $Cu^{2+}$ to the respective receptors remained stable between pH 4.5 and 12. Therefore, **8**, **9**, and **12** can be used for the estimation of $Cu^{2+}$ between pH 4.5 and 12.

### 2.4. Application of 8, 9, and 12 as logic gates[25]

Fluoroionophores **8**, **9**, and **12** have been designed according to the principles of modular PET i.e. 'receptor–spacer–fluorophore' format where the receptor and fluorophore are separated by a spacer. In simpler terms the fluorescence emission from the fluorophore is prevented when the excited state is deactivated by PET from the receptor and the receptor loses its PET donor ability when it is occupied by the matched analyte i.e. $Cu^{2+}$ here.

As we discussed earlier, in the photophysical behavior of **8**, **9**, and **12** toward metal ions and proton, either addition of $Cu^{2+}$ or decreasing the pH of the solution below pH 2.0 caused sharp enhancement of fluorescence of **8**, **9**, and **12** at 412 nm. Similar results are obtained with **8**, **9**, and **12**; the results with only **9** have been discussed. So, these inputs can be used for developing an OR logic gate (Fig. 8).[26]

The other demonstration of molecular information processing was based on a photonic AND logic gate.[27] Most of the literature reports are based on molecules, which have been designed according to the principles of PET 'receptor–spacer–fluorophore–spacer–receptor' format where the emission is observed only when both the receptors are bound to their respective analytes. Here, 'AND' logic functioning of **9** was tested in $CH_3CN$–$H_2O$ (4:1) by observing the emission spectrum under the different experimental conditions. The solutions typically tested were **9** in the presence of

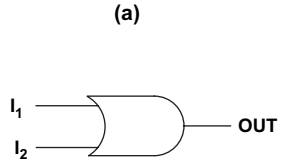


(b)

| $I_1$ $Cu^{2+}$ | $I_2$ pH | OUT 412 nm |
|---|---|---|
| 0 | 0 | 0 |
| 1 | 0 | 1 |
| 0 | 1 | 1 |
| 1 | 1 | 1 |

**Figure 8**. Molecular scale implementation of OR logic gates. (a) Logic symbol and (b) truth table (input $I_1$: state '0', $Cu^{2+}$=0 μM; state '1', $Cu^{2+}$=500 μM; input $I_2$: state '0', pH≥2; state '1', pH≤1; out: state '0', low emission; state '1', high emission).

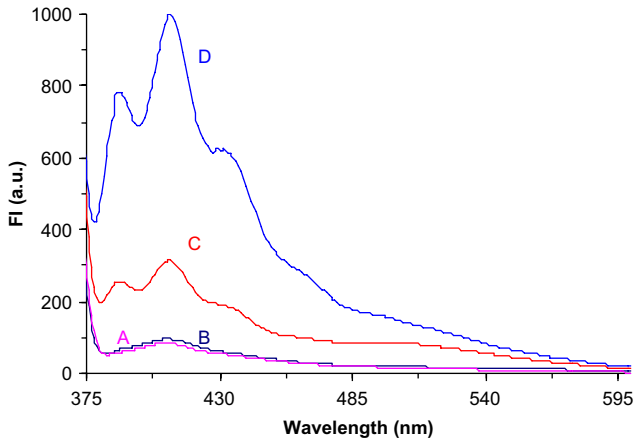


**Figure 9**. Fluorescence emission spectrum of AND logic gate of **9** in $CH_3CN$–$H_2O$ (4:1) excited at 365 nm under four experimental conditions. (A) **9**, $Cu^{2+}$=0 μM, pH=6.0; (B) **9**, pH=2.5, $Cu^{2+}$=0 μM; (C) **9**, $Cu^{2+}$=100 μM, pH=6.0; (D) **9**, $Cu^{2+}$=100 μM, pH=2.5.

(A) pH=6.0 and $Cu^{2+}$=0 μM, (B) pH=2.5 and $Cu^{2+}$=0 μM, (C) pH=6.0 and $Cu^{2+}$=100 μM, and (D) pH=2.5 and $Cu^{2+}$=100 μM (Fig. 9). The solution of free **9** has weak emission due to PET to the fluorophore. On lowering the pH to 2.5, the protonation was not affected and still a weak emission was observed. On addition of $Cu^{2+}$ at pH 6.0 a small increase in emission was observed (Figs. 9 and 10a), which is defined as the threshold value. However, on the addition of $Cu^{2+}$ at pH 2.5 the emission intensity was increased by ~200%. On addition of EDTA (100 μM), the FI was lowered back to that of **9** at pH 2.5. These results clearly show that complexation of **9** with $Cu^{2+}$ at pH 3.0 is responsible for this fluorescence enhancement and rules out the decomposition of **9** under experimental conditions.

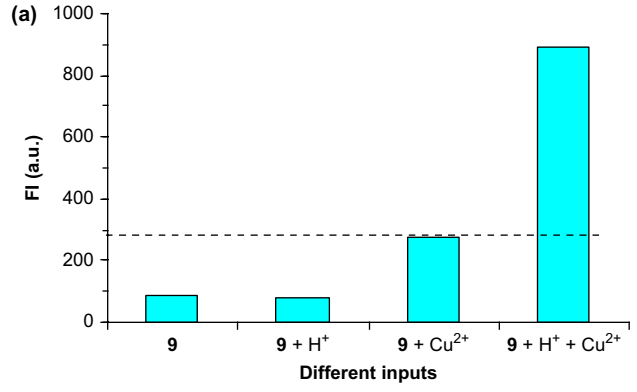


(b)

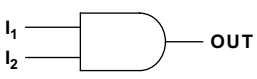


| $I_1$ $H^+$ | $I_2$ $Cu^{2+}$ | OUT 412 nm |
|---|---|---|
| 0 | 0 | 0 |
| 0 | 1 | 0 |
| 1 | 0 | 0 |
| 1 | 1 | 1 |

**Figure 10**. (a) Fluorescence intensities of **9** (5 μM, $CH_3CN$–$H_2O$ (4:1)) at 412 nm with different chemical inputs. (b) Logic symbol and truth table (input $I_1$: state '0', $Cu^{2+}$=0 μM; state '1', $Cu^{2+}$=100 μM; input $I_2$: state '0', pH=6.0; state '1', pH=2.5; out: state '0', low emission; state '1', high emission). The dashed line in **10a** marks the threshold value.

## 3. Conclusion

In conclusion, the hydrophobic environment achieved by the presence of various aromatic rings and their appropriate placement in fluorophores **3**, **8**, **9**, and **12** provides stability to their emission even when the pH is as low as 2 and their complexes above pH 4. Furthermore, moving the anthracene moiety in **3** from the center of the molecule to the termini in cases of **8**, **9**, and **12** changes the fluorescence quenching to fluorescence enhancement on addition of $Cu^{2+}$. This stability of fluorescence under acidic conditions and $Cu^{2+}$ induced fluorescence enhancement can be elaborated to construct OR and AND logic gates.

## 4. Experimental

### 4.1. General

Melting points were determined in capillaries and are uncorrected. $^1$H NMR spectra were recorded on JEOL Al 300 MHz instrument using $CDCl_3$ solution containing tetramethylsilane as an internal standard. The chemical shifts are reported in $\delta$ values relative to TMS and coupling constants ($J$) are expressed in Hertz. $^{13}$C NMR spectra were recorded at 75 MHz and the values are reported relative to $CDCl_3$ signal at $\delta$ 77.0. Chromatography was performed with silica gel 100–200 mesh and the reactions were monitored by thin layer chromatography (TLC) with glass plates coated with silica gel HF-254. 1,4-Bis(bromomethyl)benzene,[28] 1,4-bis(bromomethyl)-2,5-dimethoxybenzene,[29] and 1,4-bis-(chloromethyl)naphthalene[30] were prepared according to the literature procedures.

### 4.2. General procedure for the preparation of receptors 3, 6, 7, and 11

In a two-necked round-bottomed flask, prewashed NaH (110 mg, 4.59 mmol) was taken in dry DMF and 2-aminothiophenol (**2**) (522 mg, 4.17 mmol) was added with stirring under nitrogen at 40±2 °C. The stirring was continued. After the hydrogen evolution ceased, TBA $HSO_4$ (25–30 mg) and 9,10-bis(chloromethyl)anthracene (**1**) (500 mg, 1.81 mmol) were added and stirring was continued for 24–30 h. During this period, the reaction was completed. The suspended solid was filtered off and washed with ethyl acetate. The combined filtrate was distilled off under vacuum and the residue was triturated with methanol to get the white solid, which was crystallized from chloroform–methanol (1:1) to isolate **3**.

**4.2.1. 9,10-Bis(2-aminophenylthio)anthracene (3).** Yield: 703 mg, 85%, yellowish green, mp 186 °C ($CHCl_3$); FAB mass $m/z$ 453 ($M^+$+H); $^1$H NMR ($CDCl_3$): $\delta$ 4.63 (br s, 4H, 2×$NH_2$, exchanges with $D_2O$), 4.90 (s, 4H, 2×$SCH_2$), 6.52 (t, $J$=7.6 Hz, 2H, ArH), 6.72 (d, $J$=7.6 Hz, 2H, ArH), 7.07 (t, $J$=7.6 Hz, 2H, ArH), 7.23 (d, $J$=7.6 Hz, 2H, ArH), 7.46 (dd, 4H, $J_1$=6.8 Hz, $J_2$=3.2 Hz, ArH), 8.28 (dd, 4H, $J_1$=6.8 Hz, $J_2$=3.2 Hz, ArH); $^{13}$C NMR ($CDCl_3$): $\delta$ 32.8, 114.9, 116.6, 124.6, 125.5, 127.7, 129.7, 129.8, 130.3, 136.5, 148.7; IR $\lambda_{max}$ ($cm^{-1}$): 3477, 3363 (d, $NH_2$). Found C, 74.1; H, 5.3; N, 6.2%. $C_{28}H_{24}N_2S_2$ requires C, 74.30; H, 5.34; N, 6.19; S, 14.17%.

**4.2.2. 1,4-Bis(2-aminophenylthio)benzene (6).** Yield: 60%, mp 101–103 °C (lit. mp 104–106 °C) ($CH_2Cl_2$–MeOH); FAB mass $m/z$ 353 ($M^+$+H); $^1$H NMR ($CDCl_3$): $\delta$ 3.63 (br s, 4H, 2×$NH_2$, exchanges with $D_2O$), 3.82 (s, 4H, 2×$CH_2S$), 6.55–6.67 (m, 4H, ArH), 6.97 (s, 4H, ArH), 7.04–7.18 (m, 4H, ArH); $^{13}$C NMR (normal/DEPT-135) ($CDCl_3$): $\delta$ 39.3 (−ve, $CH_2$), 114.8 (+ve, ArCH), 117.2 (ab, ArC), 118.4 (+ve, ArCH), 128.8 (+ve, ArCH), 130.0 (+ve, ArCH), 136.5 (+ve, ArCH), 137.1 (ab, ArC), 148.6 (ab, ArC); IR $\lambda_{max}$ ($cm^{-1}$): 3465, 3367 (d, $NH_2$). Found C, 67.9; H, 5.7; N, 7.9; S, 17.95%. $C_{20}H_{20}N_2S_2$ requires C, 68.14; H, 5.72; N, 7.95; S, 18.19%.

**4.2.3. 1,4-Bis(2-aminophenylthio)-2,5-dimethoxy-benzene (7).** Yield: 70%, mp 148–149 °C ($CH_2Cl_2$–MeOH); FAB mass $m/z$ 412 ($M^+$); $^1$H NMR ($CDCl_3$): $\delta$ 3.57 (s, 6H, 2×$OCH_3$), 3.87 (s, 4H, 2×$CH_2S$), 4.23 (br s, 4H, due to $NH_2$, exchanges with $D_2O$), 6.31 (s, 2H, ArH), 6.62 (t, $J$=7.5 Hz, 2H, ArH), 6.70 (d, $J$=7.5 Hz, 2H, ArH), 7.10 (t, $J$=7.5 Hz, 2H, ArH), 7.21 (d, $J$=7.5 Hz, 2H, ArH); $^{13}$C NMR (normal/DEPT-135) ($CDCl_3$): $\delta$ 33.9 (−ve, $CH_2$), 56.0 (+ve, $OCH_3$), 113.4 (+ve, ArCH), 114.7 (+ve, ArCH), 117.5 (ab, ArC), 118.3 (+ve, ArCH), 125.9 (ab, ArC), 130.0 (+ve, ArCH), 136.9 (+ve, ArCH), 148.9 (ab, ArC), 150.4 (ab, ArC); IR $\lambda_{max}$ ($cm^{-1}$): 3470, 3367 (d, $NH_2$). Found C, 63.88; H, 5.74; N, 6.53; S, 15.41%. $C_{22}H_{24}N_2O_2S_2$ requires C, 64.05; H, 5.86; N, 6.79; S, 15.54%.

**4.2.4. 1,4-Bis(2-aminophenylthio)naphthalene (11).** Yield: 55%, white solid, mp 76–78 °C; FAB mass $m/z$ 402 ($M^+$); $^1$H NMR ($CDCl_3$): $\delta$ 3.77 (br s, 4H, 2×$NH_2$, exchanges with $D_2O$), 4.29 (s, 4H, 2×$CH_2S$), 6.57–6.65 (m, 4H, ArH,), 6.83 (s, 2H, ArH), 7.09 (t, $J$=7.5 Hz, 2H, ArH), 7.17 (d, $J$=7.5 Hz, 2H, ArH), 7.55 (dd, $J_1$=6.6 Hz, $J_2$=3.3 Hz, 2H, ArH), 8.16 (dd, $J_1$=6.6 Hz, $J_2$=3.3 Hz, 2H, ArH); $^{13}$C NMR (normal/DEPT-135) ($CDCl_3$): $\delta$ 37.7 (−ve, $CH_2$), 114.8 (+ve, ArCH), 117.6 (ab, ArC), 118.4 (+ve, ArCH), 124.6 (+ve, ArCH), 125.9 (+ve, ArCH), 126.6 (+ve, ArCH), 130.1 (+ve, ArCH), 131.6 (ab, ArC), 133.5 (ab, ArC), 136.6 (+ve, ArCH), 148.7 (ab, ArC); IR $\lambda_{max}$ ($cm^{-1}$): 3467, 3360 (d, $NH_2$). Found C, 71.87; H, 5.74; N, 6.73; S, 15.91%. $C_{24}H_{22}N_2S_2$ requires C, 71.6; H, 5.51; N, 6.96; S, 15.93%.

### 4.3. General procedure for the preparation of receptors 8, 9, and 12[31]

The solution of **6** (300 mg, 0.85 mmol) and anthracene-9-aldehyde (228 mg, 1.1 mmol) in dry THF (30 ml) containing a suspension of $MgSO_4$ (dry) (409 mg, 3.4 mmol) was stirred for 48 h at room temperature. $MgSO_4$ was filtered off and washed with dry THF. The combined filtrate was treated with $NaBH_4$ (77 mg, 2.12 mmol) and $I_2$ (216 mg, 0.85 mmol). The reaction mixture was refluxed for 36 h. This was then cooled and treated with methanolic KOH (2%, 20 ml). Then it was diluted with water and was extracted with $CH_2Cl_2$. The solvent was distilled off and the residue was purified through column chromatography over silica using $CH_2Cl_2$–hexane as an eluant to get **8**.

**4.3.1. 1-[2-(Anthracenyl-9-methylamino)phenylthiomethyl]-4-(2-aminophenylthiomethyl)benzene (8).** Yield:

20%, yellow solid, mp 121–123 °C; FAB mass *m/z* 542 ($M^+$); $^1$H NMR ($CDCl_3$): $\delta$ 3.58 (s, 2H, $CH_2S$), 3.75 (s, 2H, $CH_2S$), 4.13 (s, 2H, $NH_2$, exchanges with $D_2O$), 5.17 (br s, 2H, $CH_2N$), 5.21 (br s, 1H, NH, exchanges with $D_2O$), 6.60 (t, $J$=7.5 Hz, 1H, ArH), 6.63–6.67 (m, 2H, ArH), 6.69 (d, $J$=7.5 Hz, 2H, ArH), 6.80 (d, $J$=7.5 Hz, 2H, ArH), 7.04–7.11 (m, 2H, ArH), 7.14 (d, $J$=7.5 Hz, 1H, ArH), 7.21 (d, $J$=7.5 Hz, 1H, ArH), 7.39 (t, $J$=7.5 Hz, 1H, ArH), 7.46–7.54 (m, 4H, ArH), 8.06 (d, $J$=9.0 Hz, 2H, ArH), 8.25 (d, $J$=9.0 Hz, 2H, ArH), 8.50 (s, 1H, ArH); $^{13}$C NMR (normal/DEPT-135) ($CDCl_3$): $\delta$ 38.8 (−ve, $CH_2$), 39.4 (−ve, $CH_2$), 40.8 (−ve, $CH_2$), 110.0 (+ve, ArCH), 114.8 (+ve, ArCH), 117.0 (+ve, ArCH), 117.2 (ab, ArC), 117.3 (ab, ArC), 118.4 (+ve, ArCH), 124.1 (+ve, ArCH), 125.2 (+ve, ArCH), 126.5 (+ve, ArCH), 128.0 (+ve, ArCH), 128.6 (+ve, ArCH), 128.7 (+ve, ArCH), 129.2 (+ve, ArCH), 130.0 (+ve, ArCH), 130.5 (ab, ArC), 130.6 (+ve, ArCH), 131.5 (ab, ArC), 136.5 (+ve, ArCH), 136.6 (ab, ArC), 136.7 (+ve, ArCH), 136.9 (ab, ArC), 148.6 (ab, ArC), 149.1 (ab, ArC); IR $\lambda_{max}$ ($cm^{-1}$): 3463, 3363 ($NH_2$). Found C, 77.23; H, 5.38; N, 4.98; S, 11.61%. $C_{35}H_{30}N_2S_2$ requires C, 77.45; H, 5.57; N, 5.16; S, 11.82%.

**4.3.2. 1-[2-(Anthracenyl-9-methylamino)phenylthiomethyl]-4-(2-aminophenylthiomethyl)-2,5-dimethoxybenzene (9).** Yield 28%, yellow solid, mp 124–125 °C ($CH_2Cl_2$–MeOH); FAB mass *m/z* 602 ($M^+$); $^1$H NMR ($CDCl_3$): $\delta$ 3.11 (s, 3H, $OCH_3$), 3.40 (s, 3H, $OCH_3$), 3.65 (s, 2H, $CH_2S$), 3.79 (s, 2H, $CH_2S$), 5.19 (br s, 2H, $NH_2$, exchanges with $D_2O$), 5.21 (s, 2H, $CH_2N$), 6.14 (s, 1H, ArH), 6.18 (s, 1H, ArH), 6.59–6.70 (m, 3H, ArH), 7.06–7.19 (m, 3H, ArH), 7.31 (d, $J$=1.6 Hz, 1H, ArH), 7.48–7.54 (m, 5H, ArH), 8.06 (d, $J$=9.4 Hz, 2H, ArH), 8.27 (d, $J$=9.4 Hz, 2H, ArH), 8.51 (s, 1H, ArH); $^{13}$C NMR (normal/DEPT-135) ($CDCl_3$): $\delta$ 33.5 (−ve, $CH_2$), 34.0 (−ve, $CH_2$), 41.0 (−ve, $CH_2$), 55.5 (+ve, $OCH_3$), 55.8 (+ve, $OCH_3$), 109.9 (+ve, ArCH), 113.2 (+ve, ArCH), 114.7 (+ve, ArCH), 116.9 (+ve, ArCH), 117.5 (ab, ArC), 117.6 (ab, ArC), 118.2 (+ve, ArCH), 124.1 (+ve, ArCH), 125.2 (+ve, ArCH), 125.3 (ab, ArC), 125.8 (ab, ArC), 126.5 (+ve, ArCH), 127.9 (+ve, ArCH), 129.1 (+ve, ArCH), 129.2 (ab, ArC), 129.9 (+ve, ArCH), 130.5 (+ve, ArCH), 130.6 (ab, ArC), 131.5 (ab, ArC), 136.9 (+ve, ArCH), 137.0 (+ve, ArCH), 148.8 (ab, ArC), 149.4 (ab, ArC), 150.3 (ab, ArC), 150.5 (ab, ArC); IR $\lambda_{max}$ ($cm^{-1}$): 3429, 3380, 3334 ($NH_2$). Found C, 73.57; H, 5.52; N, 4.52; S, 10.47%. $C_{37}H_{34}N_2O_2S_2$ requires C, 73.72; H, 5.69; N, 4.65; S, 10.64%.

**4.3.3. 1-[2-(Anthracenyl-9-methylamino)phenylthiomethyl]-4-(2-aminophenylthiomethyl)naphthalene (12).** Yield: 27%, yellow solid, mp 135–137 °C; FAB mass 592 ($M^+$); $^1$H NMR ($CDCl_3$): $\delta$ 4.05 (s, 2H, $CH_2S$), 4.19 (s, 2H, $CH_2S$), 5.21 (br s, 2H, $NH_2$, exchanges with $D_2O$), 5.23 (br s, 2H, $CH_2N$), 6.56–6.69 (m, 5H, ArH), 6.97 (t, $J$=7.5 Hz, 1H, ArH), 7.05–7.15 (m, 3H, ArH), 7.24 (d, $J$=7.5 Hz, 1H, ArH), 7.32–7.44 (m, 2H, ArH), 7.46–7.53 (m, 4H, ArH), 7.75 (d, $J$=8.4 Hz, 1H, ArH), 7.99 (d, $J$=8.4 Hz, 1H, ArH), 8.08 (d, $J$=7.5 Hz, 2H, ArH), 8.27 (d, $J$=7.5 Hz, 2H, ArH), 8.54 (s, 1H, ArH); $^{13}$C NMR (normal/DEPT-135) ($CDCl_3$): $\delta$ 37.2 (−ve, $CH_2$), 37.7 (−ve, $CH_2$), 40.8 (−ve, $CH_2$), 110.1 (+ve, ArCH), 114.8 (+ve, ArCH), 117.1 (+ve, ArCH), 117.7 (ab, ArC), 118.4 (+ve, ArCH), 124.1 (+ve, ArCH), 124.3 (+ve, ArCH), 125.2 (+ve, ArCH), 125.6 (+ve, ArCH), 126.5 (+ve, ArCH), 125.7 (+ve, ArCH), 126.6 (+ve, ArCH), 126.7 (+ve, ArCH), 128.1 (+ve, ArCH), 129.2 (+ve, ArCH), 130.1 (+ve, ArCH), 130.5 (ab, ArC), 130.8 (+ve, ArCH), 131.4 (ab, ArC), 131.6 (ab, ArC), 133.4 (ab, ArC), 136.6 (+ve, ArCH), 137.0 (+ve, ArCH), 148.7 (ab, ArC), 149.3 (ab, ArC). Found C, 78.93; H, 5.33; N, 4.56; S, 10.67%. $C_{39}H_{32}N_2S_2$ requires C, 79.02; H, 5.44; N, 4.73; S, 10.82%.

### 4.4. UV–vis and fluorescence experiments

UV–vis absorption and fluorescence spectra were recorded on Shimadzu UV-1601-PC spectrophotometer and Shimadzu RF1501 spectrofluorophotometer with a 1 cm quartz cell at 25±0.1 °C. The solutions of fluoroionophores **3**, **8**, **9**, and **12** and metal nitrates were prepared in double distilled acetonitrile. A number of solutions containing **3/8/9/12** (5 μM) and different concentrations of metal nitrates were prepared and kept at 25±1 °C for 2 h before recording their absorption or fluorescence spectra. The spectra obtained were analyzed through curve fitting procedures by using SPECFIT 3.0.36 to determine the stability constants and the distribution of various species.

### 4.5. pH titration experiments

The pH titrations of **3** (5 μM), **8**, **9**, and **12** (1 μM) in $CH_3CN$–$H_2O$ (4:1 v/v) were performed with acid (HCl) to investigate the <7 pH range and in a separate experiment with base (NaOH) to investigate the >7 pH range and at regular intervals pH fluorescence spectra were recorded.

### 4.6. Experimental procedure for AND gate

Solution containing **9** (5 μM) was treated with HCl and pH of the solution was adjusted to 2.5 and fluorescence spectrum was recorded. In a separate experiment, a solution containing **9** (5 μM) and copper nitrate (100 μM) was prepared in $CH_3CN$–$H_2O$ (4:1 v/v) at pH 6.0 separately in a 50 ml measuring flask and recorded its fluorescence spectrum. Then the pH of the solution was changed with acid (HCl) and at regular intervals pH fluorescence spectra were recorded.

## Acknowledgements

We thank DST, New Delhi for the financial assistance.

## References and notes

1. (a) de Silva, A. P.; Gunaratne, H. Q. N.; Gunnlaugsson, T. A.; Huxley, T. M.; McCoy, C. P.; Rademacher, J. T.; Rice, T. E. *Chem. Rev.* **1997**, *97*, 1515–1566; (b) Czarnik, A. W. *Acc. Chem. Res.* **1994**, *27*, 302–308; (c) Fabbrizzi, L.; Poggi, A. *Chem. Soc. Rev.* **1997**, 197–202; (d) Callan, J. F.; de Silva, A. P.; Magri, D. C. *Tetrahedron* **2005**, *61*, 8551–8588.
2. Lockhart, J. C. Chemical Sensors. *Comprehensive Supramolecular Chemistry*; Gokel, G. W., Ed.; Pergamon, Elsevier Science: Oxford, 1996; Vol. 1, p 605.
3. (a) Kramer, R. *Angew. Chem., Int. Ed.* **1998**, *37*, 772–773; (b) Rurack, K.; Kollmannsberger, M.; Resch-Genger, U.; Daub,

J. *J. Am. Chem. Soc.* **2000**, *122*, 968–969; (c) Zheng, Y.; Orbulescu, J.; Ji, X.; Andreopoulos, F. M.; Pham, S. M.; Leblanc, R. M. *J. Am. Chem. Soc.* **2003**, *125*, 2680–2686; (d) Ghosh, P.; Bharadwaj, P. K.; Mandel, S.; Ghosh, S. *J. Am. Chem. Soc.* **1996**, *118*, 1553–1554.

4. (a) McCord, J.; Fridovich, I. *J. Biol. Chem.* **1969**, *244*, 6049–6055; (b) Brown, D. R.; Kzolwski, H. *Dalton Trans.* **2004**, 1907–1917; (c) Valentine, J. S.; Hart, P. J. *Proc. Natl. Acad. Sci. U.S.A.* **2003**, *100*, 3617–3622; (d) Waggoner, D. J.; Bartnikas, T. B.; Gitlin, J. D. *Neurobiol. Dis.* **1999**, *6*, 221–230; (e) Vulpe, C.; Levinson, B. S.; Whitney, S.; Packman, S.; Gitscheir, J. *Nat. Genet.* **1993**, *3*, 7–13; (f) Bull, P. C.; Thomas, G. R.; Rommens, J. M.; Forbes, J. R.; Cox, D. W. *Nat. Genet.* **1993**, *5*, 327–337; (g) Barnham, K. J.; Masters, C. L.; Bush, A. I. *Nat. Rev. Drug Discov.* **2004**, *3*, 205–214.
5. Fabbrizzi, L.; Licchelli, M.; Pallavicini, P.; Perotti, A.; Sacchi, D. *Angew. Chem., Int. Ed. Engl.* **1994**, *33*, 1975–1977.
6. Fabbrizzi, L.; Licchelli, M.; Pallavicini, P.; Perotti, A.; Taglietti, A.; Sacchi, D. *Chem.—Eur. J.* **1996**, *2*, 75–82.
7. Torrado, A.; Walkup, G. K.; Imperiali, B. *J. Am. Chem. Soc.* **1998**, *120*, 609–610.
8. Zheng, Y.; Huo, Q.; Kele, P.; Andreopoulos, F. M.; Pham, S. M.; Lablanc, R. M. *Org. Lett.* **2001**, *3*, 3277–3280.
9. Bhattacharya, S.; Thomas, M. *Tetrahedron Lett.* **2000**, *41*, 10313–10317.
10. Singh, A.; Yao, Q.; Tong, L.; Still, W. C.; Sames, D. *Tetrahedron Lett.* **2000**, *41*, 9601–9605.
11. Bodenant, B.; Weil, T.; Pourcel, M. B.; Fages, F.; Barbe, B.; Pianet, I.; Laguerre, M. *J. Org. Chem.* **1999**, *64*, 7034–7039.
12. Beltramello, M.; Gatos, M.; Mancin, F.; Tecilla, P.; Tonellato, U. *Tetrahedron Lett.* **2001**, *42*, 9143–9146.
13. Zhang, W.-C.; Zhu, Y.; Li, E.-C.; Liu, T.-J.; Huang, Z.-T. *Tetrahedron* **2000**, *56*, 3365–3371.
14. De Santis, G.; Fabbrizzi, L.; Licchelli, M.; Mangano, C.; Sacchi, D.; Sardone, N. *Inorg. Chim. Acta* **1997**, *257*, 69–76.
15. (a) Sasaki, D. Y.; Shnek, D. R.; Pack, D. W.; Arnold, F. H. *Angew. Chem., Int. Ed. Engl.* **1995**, *34*, 905–907; (b) Li, Y.; Yang, C. M. *Chem. Commun.* **2003**, 2884–2885; (c) Boiocchi, M.; Fabbrizzi, L.; Licchelli, M.; Sacchi, D.; Vazquez, M.; Zampa, C. *Chem. Commun.* **2003**, 1812–1813; (d) Zheng, Y.; Gattas-Asfura, K. M.; Konka, V.; Leblanc, R. M. *Chem. Commun.* **2002**, 2350–2351; (e) Zheng, Y.; Cao, X.; Orbulescu, J.; Konka, V.; Andreopoulos, F. M.; Pham, S. M.; Leblanc, R. M. *Anal. Chem.* **2003**, *75*, 1706–1712; (f) Mei, Y.; Bentley, P. A.; Wang, W. *Tetrahedron Lett.* **2006**, *47*, 2447–2449.
16. (a) Xiang, Y.; Tong, A.; Jin, P.; Ju, Y. *Org. Lett.* **2006**, *8*, 2863–2866; (b) Martinez, R.; Zapata, F.; Caballero, A.; Espinosa, A.; Tarraga, A.; Molina, P. *Org. Lett.* **2006**, *8*, 3235–3238; (c) Jun, E. J.; Won, H. N.; Kim, J. S.; Lee, K.-H.; Yoon, J. *Tetrahedron Lett.* **2006**, *47*, 4577–4580; (d) Wen, Z.-C.; Yang, R.; He, H.; Jiang, Y.-B. *Chem. Commun.* **2006**, 106–108; (e) Xu, Z.; Xiao, Y.; Qian, X.; Cui, J.; Cui, D. *Org. Lett.* **2005**, *7*, 889–892.
17. (a) Kaur, S.; Kumar, S. *Tetrahedron Lett.* **2004**, *45*, 5081–5085; (b) Kumar, S.; Kaur, P.; Kaur, S. *Tetrahedron Lett.* **2002**, *43*, 1097–1099; (c) Kaur, S.; Kumar, S. *Chem. Commun.* **2002**, 2840–2841.
18. (a) Romero, A.; Nar, H.; Huber, R.; Messerschmidt, A.; Kalverda, A. P.; Canters, D. R.; Mathews, F. S. *J. Mol. Biol.* **1994**, *236*, 1196–1211; (b) Botuyan, M. V.; Toy-Palmer, A.; Chung, J.; Blake, R. C., II; Beroza, P.; Case, D. H. J. *J. Mol. Biol.* **1996**, *263*, 752–767; (c) Guss, J. M.; Merritt, E. A.; Phizackerley, R. P.; Freeman, H. C. *J. Mol. Biol.* **1996**, *262*, 686–705.
19. (a) Baker, E. N. *J. Mol. Biol.* **1988**, *203*, 1071–1095; (b) Hay, M.; Richards, J. H.; Lu, Y. *Proc. Natl. Acad. Sci. U.S.A.* **1996**, *93*, 461–464; (c) Buning, C.; Comba, P. *Eur. J. Inorg. Chem.* **2000**, 1267–1273 and references therein; (d) Buning, C.; Canters, G. W.; Comba, P.; Dennison, C.; Jeuken, L.; Melter, M.; Sanders-Loehr, J. *J. Am. Chem. Soc.* **2000**, *122*, 204–211 and references therein.
20. Miller, M. W.; Amidon, R. W.; Tawney, P. O. *J. Am. Chem. Soc.* **1955**, *77*, 2845–2848.
21. Kumar, S.; Kaur, S.; Singh, H. *J. Inclusion Phenom. Macrocycl. Chem.* **2001**, *39*, 277–283.
22. Initially fluorescent titration was carried out by excitation at $\lambda_{max}$ 395 nm, which seems to be the isosbestic point during the metal titration spectrophotometrically, but fluorescence intensity was very weakly observed. So, we prefer to use $\lambda_{max}$ of the highest intensity band i.e. 365 nm in the UV spectrum, for excitation.
23. Lange, N. A. *Lange's Handbook of Chemistry*, 13th ed.; Dean, J. A., Ed.; McGraw-Hill: New York, NY, 1985; pp 3–139.
24. There is the possibility that species $[CuL]^{2+}$ or ML type may exist, however, when ML was included in the hypothesized set of species present in the solution of the fluorescence data refinement, the data processing discarded it, excluding its presence. Also, as the fluorescence titration showed that nearly 500 μM $Cu^{2+}$ is required to effect the complete enhancement of the fluorescence so the formation of ML species may not be observable in these titrations.
25. (a) Raymo, F. M. *Adv. Mater.* **2002**, *14*, 401–414 and references therein; (b) de Silva, A. P.; Gunnaratne, H. Q. N.; McCoy, C. P. *Nature* **1993**, *364*, 42–44; (c) *Molecular Switches*; Feringa, B. L., Ed.; Wiley-VCH: Weinheim, 2001.
26. (a) de Silva, A. P.; de Silva, S. A. *J. Chem. Soc., Chem. Commun.* **1986**, 1709–1710; (b) de Silva, A. P.; Gunnaratne, H. Q. N.; Maguire, G. E. M. *J. Chem. Soc., Chem. Commun.* **1994**, 1213–1215.
27. (a) de Silva, A. P.; Gunnaratne, H. Q. N.; McCoy, C. P. *J. Am. Chem. Soc.* **1997**, *119*, 7891–7892; (b) Magri, D. C.; Coen, G. D.; Boyd, R. L.; de Silva, A. P. *Anal. Chim. Acta* **2006**, *568*, 156–160; (c) Magri, D. C.; Brown, G. J.; McClean, G. D.; de Silva, A. P. *J. Am. Chem. Soc.* **2006**, *128*, 4950–4951.
28. Wilhelm, W. *J. Org. Chem.* **1952**, *17*, 523–528.
29. Van der Made, A. W.; Van der Made, R. H. *J. Org. Chem.* **1993**, *58*, 1262–1263.
30. Hanhela, P. J.; Paul, D. B. *Aust. J. Chem.* **1989**, *42*, 287–299.
31. McKennon, M. J.; Meyers, A. I.; Drauz, K.; Schwarm, M. *J. Org. Chem.* **1993**, *58*, 3568–3571.